BJPsych | The British Journal of Psychiatry (2015) 207, 143–148. doi: 10.1192/bjp.bp.114.151654

Specific effect of the fragile-X mental retardation-1 gene (*FMR1*) on white matter microstructure

Tamar Green,* Naama Barnea-Goraly,* Mira Raman, Scott S. Hall, Amy A. Lightbody, Jennifer L. Bruno, Eve-Marie Quintin and Allan L. Reiss

Background
Fragile-X syndrome (FXS) is a neurodevelopmental disorder associated with intellectual disability and neurobiological abnormalities including white matter microstructural differences. White matter differences have been found relative to neurotypical individuals.

Aims
To examine whether FXS white matter differences are related specifically to FXS or more generally to the presence of intellectual disability.

Method
We used voxel-based and tract-based analytic approaches to compare individuals with FXS ($n = 40$) with gender- and IQ-matched controls ($n = 30$).

Results
Individuals with FXS had increased fractional anisotropy and decreased radial diffusivity values compared with IQ-matched controls in the inferior longitudinal, inferior fronto-occipital and uncinate fasciculi.

Conclusions
The genetic variation associated with FXS affects white matter microstructure independently of overall IQ. White matter differences, found in FXS relative to IQ-matched controls, are distinct from reported differences relative to neurotypical controls. This underscores the need to consider cognitive ability differences when investigating white matter microstructure in neurodevelopmental disorders.

Declaration of interest
T.G., N.B.G., M.M.R., S.S.H., A.A.L., J.L.B. and E.M.Q.: None. A.L.R. reports personal fees from Genentech/Roche, outside the submitted work.

Fragile-X syndrome (FXS), arising from a full mutation in the fragile-X mental retardation-1 (*FMR1*) gene,[1] is the most common inherited single-gene cause of intellectual disability[2] and an important risk factor for autistic behaviour.[3] White matter microstructural differences have been observed between individuals with FXS and neurotypical controls (individuals without any known psychological or learning disorder). Individuals with FXS have lower fractional anisotropy,[4] and higher radial diffusivity and axial diffusivity[5] values relative to neurotypical controls. However, correlations between white matter microstructure and cognitive abilities indicate that lower fractional anisotropy values are associated with lower cognitive abilities in general.[6] Thus, differences in white matter microstructure previously found between FXS and neurotypical controls are potentially confounded by differences in overall cognitive ability. Our study was designed specifically to examine the effects of the *FMR1* full mutation without this confound.

FXS is caused by expanded trinucleotide repeats on the long arm of the X chromosome. These repeats are prone to hypermethylation and consequent silencing of the *FMR1* gene,[1] resulting in reduced expression of fragile-X mental retardation protein (FMRP).[7] FMRP plays a central role in synaptic plasticity, protein translation,[8] axonal growth and guidance,[9] and synaptogenesis.[10] FMRP has also been implicated in regulation of myelin basic protein mRNA in oligodendrocytes[11] and myelin formation.[12] Studies of the *FMR1* knockout mouse model have shown aberrant axonal growth, synaptogenesis and myelin formation that may underlie observed white matter structural differences found in diffusion tensor imaging (DTI) studies of humans with FXS.[4,5,13] Currently, significant effort is being devoted to the development of disease-specific pharmacological treatments in humans with FXS, thereby increasing the demand for sensitive and accurate biomarkers that can be used in clinical trials, including those derived from human neuroimaging.[14] Thus, elucidation of the specific connection between downstream effects of the *FMR1* mutation and white matter microstructure in FXS beyond general associations with cognitive ability holds promise for providing such biomarkers.

In this study we sought to investigate white matter microstructural differences between adolescent and young adult males and females with FXS and gender- and IQ-matched controls (IQ-CTL) with idiopathic developmental disabilities. In addition to IQ, the groups were also matched on measures of adaptive and autistic behaviour. We used voxel-based and tract-based analytic approaches to compare groups and also performed within-group correlations between adaptive behaviour as measured by Vineland Adaptive Behavior Scales[15] and white matter microstructure, and examined between-group interactions for these brain–behaviour correlations. Our overarching hypothesis was that measures of white matter microstructure would yield significant differences between an FXS group and an IQ-CTL group, further specifying the influence of FXS status on white matter neuroanatomy.

Method

Participants and testing

Data presented here are part of a prospective, longitudinal study funded by the National Institute of Mental Health. The study included the following groups: FXS and IQ-CTL (Table 1). The diagnosis of FXS was confirmed by Southern blot DNA analysis (Kimball Genetics, Inc.). All participants in the IQ-CTL group tested negative for FXS, as identified by a rapid polymerase chain reaction-based screening method for identification of expanded

*These authors contributed equally to the work.

https://doi.org/10.1192/bjp.bp.114.151654 Published online by Cambridge University Press

alleles of the *FMR1* gene.[16] IQ-CTL participants were group-matched to the FXS participants for gender, general intellectual level and scores from the Autism Diagnostic Observation Schedule (ADOS)[17] and Vineland Adaptive Behavior Scales, second edition[15] (Table 1). Participant medications were grouped into three classes: (a) antidepressants, (b) stimulants and (c) antipsychotics, anticonvulsants and other psychoactive drugs (Table 1).

Exclusion criteria for all groups included premature birth (gestational age under 34 weeks), low birth weight (less than 2000 g), known diagnosis of a major psychiatric or current neurological disorder including seizures, and any contra-indications for a magnetic resonance imaging (MRI) scan. All participants underwent cognitive evaluation conducted by trained psychologists, using the age-appropriate versions of either the Wechsler Intelligence Scale for Children-III or the Abbreviated Scale of Intelligence.[18,19] Autistic symptoms in the FXS and IQ-CTL groups were assessed using the ADOS.[17] Adaptive behaviour was assessed in the FXS and IQ-CTL groups, using the Vineland Adaptive Behavior Scales. Participants with FXS were recruited through the National Fragile-X Foundation, a local network of physicians, and advertisement on the Stanford University School of Medicine website. Participants in the IQ-CTL group were recruited through California regional centres and community organisations, and by word of mouth. Stanford University's research ethics board approved the study and participants gave their informed written consent. Informed written consent from guardians as well as written assent from participants was obtained for minors and for adults under guardianship.

Table 1 Demographic and cognitive measures

	TBSS analysis		
	FXS	IQ-CTL	*P*
Total, *n*	40	30	
Female, *n* (%)	25 (62.5)	17 (56.7)	NS
Medications (any), *n* (%)	19 (47.5)	11 (36.7)	NS
Antidepressants	7 (17.5)	2 (6.7)	NS[d]
Stimulants	10 (25)	9 (30)	NS
Antipsychotics	7 (17.5)	1 (3.3)	NS[d]
Age, mean (s.d.)	21.3 (3.0)	19.3 (2.8)	0.008[e]
FSIQ, mean (s.d.)	74.2 (20.4)	71.0 (19.5)	NS[e]
PIQ	74.2 (19.8)	73.4 (19.8)	NS[e]
VIQ	78.2 (19.7)	73.2 (18.3)	NS
ADOS, mean (s.d.)			
Communication[a]	1.7 (1.6)	1.6 (1.9)	NS[e]
Social[a]	4.3 (3.9)	4.3 (3.2)	NS[e]
Communication-social[a]	6.0 (5.0)	6.0 (4.7)	NS[e]
Stereotyped behaviour[b]	0.3 (0.6)	0.2 (0.5)	NS[e]
Play[c]	0.8 (0.8)	1.1 (0.9)	NS[e]
Vineland, mean (s.d.)			
Communication	64.5 (22.1)	62.5 (16.1)	NS[e]
Socialisation	74.3 (18.8)	70.4 (15.8)	NS
Daily living skills	71.5 (14.1)	68.3 (12.4)	NS
Total Adaptive Behavior	68.1 (16.1)	65.1 (12.5)	NS

FSIQ, full-scale IQ; PIQ, performance IQ; VIQ, verbal IQ; ADOS, Autism Diagnostic Observation Schedule; Vineland, Vineland Adaptive Behavior Scales, second edition; NS, not significant.
a. IQ-CTL ($n = 23$), FXS ($n = 33$).
b. IQ-CTL ($n = 22$), FXS ($n = 32$).
c. IQ-CTL ($n = 23$), FXS ($n = 32$).
d. Fisher's correction for chi-square was used because there were counts fewer than 5.
e. Data were not normally distributed, a non-parametric Mann-Whitney (Wilcoxon rank sum) test was used to compare between groups.

Diffusion tensor imaging

DTI is a neuroimaging method that assesses white matter microstructure by characterising the movement of water molecules. DTI findings are commonly reported in terms of scalars such as fractional anisotropy, radial diffusivity, and axial diffusivity. Fractional anisotropy is thought to reflect fibre diameter and density, myelination and intravoxel fibre-tract coherence; increases in these measures would increase the observed fractional anisotropy. In addition, fractional anisotropy is thought to reflect extracellular diffusion and intravoxel spacing, and increases in these measures would decrease observed fractional anisotropy.[20] Radial diffusivity, the mean of the diffusivities perpendicular to the main axis of diffusion, is thought to represent the degree of myelination; in this measure, more myelin would decrease radial diffusivity values.[21] Axial diffusivity, a measure of water diffusivity along the main axis of diffusion within a voxel, is thought to reflect fibre coherence and microstructure of axonal membranes (increases in which would increase axial diffusivity), as well as microtubules, neurofilaments and axonal branching (increases in which would decrease axial diffusivity).[21]

Image acquisition and processing

All participants were scanned in a 3T GE Signa Excite scanner at the Lucas Center for Neuroimaging, Stanford University, using one of the two custom single-channel transmit-receive quadrature head coils (one head coil was decommissioned midway through the study). Thirty-five participants (24 FXS, 11 IQ-CTL) were scanned between 2007 and 2010 with the first head coil (C. Hayes, PhD, University of Washington, Seattle, USA) and 35 participants (16 FXS and 19 IQ-CTL) were scanned between 2010 and 2011 with the second head coil (R. Hashoian, Clinical MR Solutions, Brookfield, Wisconsin, USA).

The diffusion-weighted protocol consisted of six repetitions of axially acquired images along 23 non-collinear diffusion directions ($B = 850\ s/mm^2$) and one reference image acquired without diffusion weighting ($B = 0$). Imaging parameters consisted of an image matrix of $128 \times 128 \times 44$ slices, image resolution of $1.875\ mm \times 1.875\ mm \times 3.2\ mm$, TR = 5400 ms, TE = 70.3 ms, bandwidth = 3906.25 Hz/pixel (TR, repetition time; TE, echo time). In the same session, structural T1-weighted images were acquired in the coronal plane, using a 3D volumetric spoiled gradient echo (SPGR) sequence with slices adjusted to a thickness of 1.5–1.7 mm (in order to accommodate the whole brain) with TR = 35 ms, TE = 6 ms, flip angle = 45°, field of view = $240 \times 240\ mm^2$, matrix size = $256 \times 256 \times 124$ and in-plane resolution = $0.94\ mm^3$.

Diffusion-weighted images (DWIs) were inspected for artefacts, using DTI studio (www.mristudio.org). Diffusion-weighted scans were rated as usable if a visual review revealed no artefacts or if artefacts were small and did not affect surrounding images (in which case, the images with artefacts were removed from further calculations). No more than four images (out of the six repetitions) per direction per slice were excluded.[4] There was no significant difference in the percentage of images removed between the groups ($P > 0.10$).

Tract-Based Spatial Statistics (TBSS) analysis

TBSS is a whole-brain voxel-wise analysis[22] that uses non-linear registration followed by alignment to invariant tract representation (the mean fractional anisotropy skeleton) as a way to reliably align fractional anisotropy images from multiple participants.[22,23] For our analysis, all usable DTI scans were processed using DTI studio (www.mristudio.org) and the Functional MRI Brain (FMRIB) Software Library (FSL 4.1.8; www.fmrib.ox.ac.uk/fsl/) to generate whole-brain maps of fractional anisotropy, radial diffusivity and axial diffusivity.

https://doi.org/10.1192/bjp.bp.114.151654 Published online by Cambridge University Press

TRActs Constrained by UnderLying Anatomy (TRACULA) analysis

This approach allows for the investigation of group differences within each major white matter pathway. All slices determined to be usable in DTI studio were averaged across repetitions to yield a single 23-direction DWI data-set. DWI was used as the input for diffusivity analysis in TRACULA for each participant, as implemented in the FreeSurfer 5.1 suite of software (http://surfer.nmr.mgh.harvard.edu). T1-weighted images were processed using the standard cross-sectional FreeSurfer 5.0. The technical details of the FreeSurfer procedures used are extensively described in prior publications.[24] Briefly, surface definition follows intensity gradients to optimally place the grey–white and pial surfaces at the location where the greatest shift in intensity defines the transition to another tissue class. The grey–white and pial surfaces are then visually inspected, and when needed, appropriate manual corrections are performed as per the FreeSurfer Tutorial (http://surfer.nmr.mgh.harvard.edu/fswiki/FsTutorial). All image editors are trained to achieve inter-rater reliability of $\geqslant 0.95$ (intraclass correlation coefficient) for volumetric regions of interest, using gold standard data-sets developed in our laboratory.

DWI images were processed in the TRACULA stream of FreeSurfer 5.1.[25] Briefly, the TRACULA pipeline used for this analysis included FSL's eddy current correction, $B=0$ image registration to the cross-sectional T1 image using FMRIB's Linear Image Registration Tool (FLIRT) and tensor fitting using DTFIT (fits a diffusion tensor model at each voxel).[26] Once registrations were completed, 18 major white matter pathways were reconstructed and labelled.[27] For each tract we used weighted average over the entire support of the tract distribution for the fractional anisotropy, radial diffusivity and axial diffusivity.

Statistical analyses

Given that the number of participants scanned with each head coil differed between groups (FXS *v.* IQ-CTL ($\chi^2=3.73$, $P=0.053$), TRACULA FXS *v.* IQ-CTL ($\chi^2=5.43$, $P=0.02$)) and that the groups were not fully matched for age (FXS *v.* IQ-CTL groups; see Tables 1 and 2), we included head coil type and age as covariates in all between-group comparisons.

TBSS analyses

Whole-brain voxel-wise analyses were performed in FSL 5.0.5, using TBSS.[28] General linear models were created to investigate within-group whole-brain associations (regression analyses) with behavioural measures. General linear models were then created to investigate between-group differences in brain–behaviour correlations for regions significantly correlated with behavioural measurements. Statistical analyses of the data were performed using Threshold-Free Cluster Enhancement and permutation analyses implemented in FSL 5.0.5 ('randomise', 10 000 permutations).[29] All significant statistical analyses are reported for $P<0.05$ and were individually corrected via family-wise error.

Table 2 Demographic and cognitive measures

	TRACULA analysis		
	FXS	IQ-CTL	*P*
Total, *n*	35	24	
Female, *n* (%)	23 (65.7)	14 (58.3)	NS
Age, mean (s.d.)	21.8 (2.8)	19.3 (2.9)	0.002[a]
FSIQ, mean (s.d.)	75.0 (21.6)	73.3 (21.2)	NS[a]
PIQ, mean (s.d.)	75.3 (20.6)	75.6 (20.9)	NS
VIQ, mean (s.d.)	78.6 (20.9)	75.3 (19.5)	NS

FSIQ, full-scale IQ; PIQ, performance IQ; VIQ, verbal IQ.
a. Data were not normally distributed, a non-parametric test (Mann-Whitney (Wilcoxon rank sum) test) was used to compare between groups.

TRACULA analysis

In this confirmatory analysis, we included major white matter pathways that differed between FXS and IQ-CTL groups in the TBSS analysis. We performed statistical analyses using SPSS software version 21 and R (http://www.r-project.org). Statistical analysis was performed using an analysis of covariance (ANCOVA) model with group (FXS *v.* IQ-CTL) as a between-group factor; TRACULA derived major white matter pathways as the dependent variable and age and head coil type as covariates. All data were examined for normality, predictor variable and covariate independence and homogeneity of variance to confirm the assumptions of ANCOVA. When the basic assumptions of ANCOVA were violated, we used robust ANCOVA[30] as implemented in the R project for statistical computing (http://www.r-project.org). Significant results for the TRACULA analysis are reported for $P\leqslant 0.05$, false discovery rate-corrected.

Results

Between-group TBSS analyses

Of the 78 images acquired, 7 were unusable (FXS = 5, IQ-CTL = 2). Final analyses of all usable scans included 40 participants with FXS (mean age 21.3 (s.d. = 3.0)), 25 females) and 30 IQ-CTL participants (mean age 19.3 (s.d. = 2.8)), 17 females; Table 1).

Comparison 1: FXS group *v.* IQ-CTL group

A between-group comparison revealed higher fractional anisotropy values and lower radial diffusivity values (online Fig. DS1) across several white matter pathways in the FXS group when compared with the IQ-CTL group. Both the fractional anisotropy and radial diffusivity differences were observed bilaterally throughout the superior and middle temporal gyri portions of the inferior longitudinal fasciculus (ILF) and in the regions where the ILF mingles with the inferior fronto-occipital fasciculus (IFOF; fractional anisotropy, left $t=5.11$, right $t=4.81$; radial diffusivity, left $t=-5.2$, right $t=-4.81$; all $P<0.05$ corrected) and the associate uncinate fasciculus (fractional anisotropy, left $t=5.11$, right $t=4.81$; radial diffusivity, left $t=-5.2$, right $t=-3.57$; all $P<0.05$ corrected). Higher fractional anisotropy values were detected bilaterally in the frontal regions of the IFOF (left $t=5.11$, right $t=4.81$, $Ps<0.05$ corrected), cingulate gyrus and along the corpus callosum ($t=4.86$, $P<0.05$ corrected) including forceps minor ($t=2.65$, $P<0.05$ corrected) and major ($t=4.86$, $P<0.05$ corrected; Fig. 1) and in the right superior longitudinal fasciculus (SLF; $t=3.61$, $P<0.05$ corrected). We found no significant differences in axial diffusivity between the groups. In order to assess the possible effect of medication regimens on our results, we performed a sub-analysis for which we included head coil, age and use of any psychoactive medication (Table 1) as covariates in the between-group comparison. The results for this analysis were the same as the primary between-group comparison for fractional anisotropy values. Radial diffusivity values were lower across the same white matter pathways in the FXS group when compared with the IQ-CTL group but the differences between groups only approached significance ($P=0.06$).

Given the more severe phenotype in males with FXS compared with females with FXS,[2] we conducted a male-only subgroup analysis comparing 15 males with FXS to 13 males in the IQ-CTL group. These male-only groups were matched for

https://doi.org/10.1192/bjp.bp.114.151654 Published online by Cambridge University Press

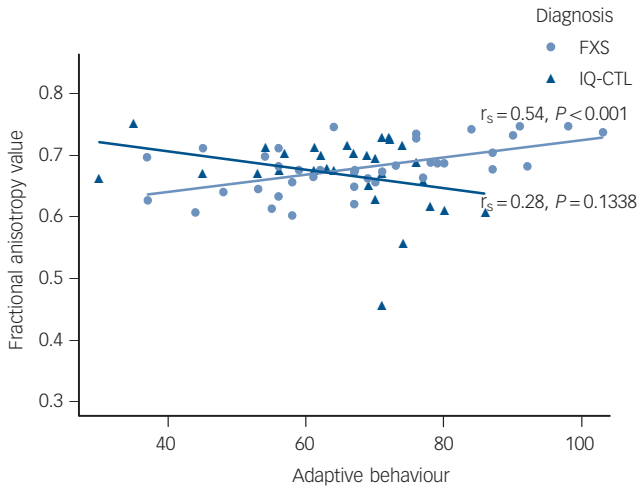

Fig. 1 Relationship between mean fractional anisotropy values in the left inferior longitudinal fasciculus, corona radiata and splenium of the corpus callosum and Vineland Adaptive Behavior scores in FXS and IQ-CTL groups.

A regression line estimating the overall trend of the data was added for illustration purposes. FXS, fragile-X syndrome; IQ-CTL, IQ-matched controls; r_s = Spearman correlation coefficient.

full-scale IQ (FSIQ; FXS mean 60.8 (s.d. = 7.2) *v.* IQ-CTL mean 65.8 (s.d. = 12.1), $P = 0.202$) and head coil ($\chi^2 = 0.51$, $P = 0.48$) but not matched for age (FXS mean 21.4 (s.d. = 2.9) *v.* IQ-CTL mean 18.8 (s.d. = 2.8), $P = 0.024$). We found no significant differences in fractional anisotropy, radial diffusivity or axial diffusivity between these male subgroups when controlling for age.

Between-group TRACULA analysis

The analysis included 35 participants with FXS (mean age 20.7 (s.d. = 2.5), 15 females) and 24 IQ-CTL participants (mean age 19.3 (s.d. = 2.9), 14 females) matched for gender and IQ (Table 2). Eleven participants were eliminated from the TRACULA analysis, eight participants because of artefacts in their T1-weighted images that precluded adequate structural results from the FreeSurfer pipeline and three because of artefacts created during the processing of the DWI average image in the TRACULA stream. An ANCOVA revealed significant differences in left ILF between the FXS and IQ-CTL groups for both fractional anisotropy and radial diffusivity values ($P < 0.05$, FDR corrected). Specifically, within the left ILF, fractional anisotropy values were higher in the FXS group when compared with the IQ-CTL group ($t = 3.51$, $P < 0.001$ uncorrected), whereas radial diffusivity values were lower in the FXS group when compared with the IQ-CTL group ($t = -3.89$, $P < 0.001$ uncorrected).

Behaviour-microstructure correlations

Within the FXS group, the Total Adaptive Behavior Composite score from the Vineland Adaptive Behavior Scales was positively correlated with fractional anisotropy values in the left ILF ($t = 5.99$, $P < 0.05$ corrected), bilateral corona radiata tracts including the body and splenium of the corpus callosum (left $t = 5.99$, right $t = 4.36$; all $P < 0.05$ corrected) and right anterior thalamic radiation ($t = 4.02$, $P < 0.05$ corrected; Fig. DS2). Total Adaptive Behavior Composite scores were negatively correlated with radial diffusivity in corona radiata tracts including the splenium of the corpus callosum bilaterally (left $t = -4.62$, right $t = -4.32$, all $P < 0.05$ corrected) and left anterior thalamic radiation ($t = -4.84$, $P < 0.05$ corrected; Fig. DS2). There were no significant correlations with adaptive behaviour and fractional anisotropy/radial diffusivity in the IQ-CTL group. Significant differences between FXS and IQ-CTL groups were detected for fractional anisotropy correlations with Total Adaptive Behavior Composite score in the left corona radiata ($t = 2.9$, $P < 0.05$ corrected) and splenium of the corpus callosum ($t = 4.2$, $P < 0.05$ corrected) and in a small cluster in the left ILF ($t = 4.2$, $P < 0.05$ corrected; Fig. 1).

Discussion

We compared white matter microstructure in adolescents and young adults with FXS to an IQ-CTL group, using voxel-based and tract-based analytic approaches. Results showed that, relative to IQ-CTLs, individuals with FXS exhibited differences in white matter microstructure as measured by DTI. In contrast to previous studies using comparisons to neurotypical controls, the FXS group showed increased fractional anisotropy and reduced radial diffusivity values in the ILF, IFOF and uncinate fasciculus and increased fractional anisotropy in the corpus callosum.[4,5] In this study, we chose to use TRACULA (tract-based) as a complementary analysis to TBSS (voxel-based) to corroborate our findings. The TRACULA analysis showed increased fractional anisotropy values and reduced radial diffusivity values in the left ILF, in the FXS group, compared with the IQ-CTL group. Significant between-group interactions were observed for brain-behaviour correlations of Total Adaptive Behavior Composite scores in the left ILF, corona radiata and splenium of the corpus callosum (fractional anisotropy), such that fractional anisotropy values were positively associated with Total Adaptive Behavior Composite scores in the FXS group, whereas fractional anisotropy values were not associated with Total Adaptive Behavior Composite scores in the IQ-CTL group (Fig. DS2). An interaction analysis demonstrated that the relationships between fractional anisotropy and adaptive behaviour were significantly different between the groups.

Our results indicate that the downstream effects of the genetic variation associated with FXS affects white matter microstructure and are independent of overall IQ effects. The between-group differences include higher fractional anisotropy and lower radial diffusivity in the FXS group compared with the IQ-CTL group in several brain regions. These findings are in contrast with previous studies where lower fractional anisotropy[4] and higher radial diffusivity and axial diffusivity[5] were reported for these regions in individuals with FXS compared with neurotypical controls. This discrepancy could be explained, at least in part, by significant correlations previously reported between white matter microstructure and cognitive abilities. Specifically, positive correlations between fractional anisotropy values and IQ scores were found in adults with intellectual disability,[6] children with very low birth weight,[31] neurotypical children[32] and gifted children.[33] It is possible that previous observations of lower fractional anisotropy in individuals with FXS when compared with neurotypical controls may be partly associated with the cognitive differences between the groups, leading to the observation of higher fractional anisotropy values in neurotypical controls. The results of our study extend knowledge beyond this observation by indicating that specific genetic influences on white matter microstructure occur in individuals with FXS, and that these influences do not appear to be driven by between-group differences in overall cognitive function.

We observed a combination of higher fractional anisotropy values and lower radial diffusivity values in the FXS group

https://doi.org/10.1192/bjp.bp.114.151654 Published online by Cambridge University Press

compared with the IQ-CTL group (Fig. DS1), using complementary image analyses methods. Axon growth dysregulation in the FXS group might lead to increased fibre density, resulting in increased fractional anisotropy and reduced radial diffusivity compared with the IQ-CTL group. There is evidence that FMRP is involved in axon guidance; specifically, FMRP regulates the axon guidance factor Semaphorin-3A (Sema3A), which is important for establishing correct pathways in the developing nervous system through collapse induction of growth cones (extension of a developing axon).[34,35] The collapse of growth cones is attenuated in *FMR1* knockout mice because of the absence of FMRP regulatory effects on Sema3A.[9] It is possible that this disturbance in axon growth regulation leads to increased fibre density in the FXS group. This hypothesis is consistent with our finding of increase fractional anisotropy and reduced radial diffusivity in similar locations across different image analyses methods (namely the ILF). Our results are also consistent with previous findings of increased fibre density in male toddlers with FXS compared with controls[13] and with the structural finding of increased white matter in the temporal lobe in FXS,[36] a brain region through which the ILF is known to traverse.

In addition to our primary analyses, a sub-analysis controlling for the use of psychotropic medications revealed similar results for fractional anisotropy values and approached significance for radial diffusivity values in the same white matter locations. It is possible that controlling for psychotropic medications, in addition to age and head coil, reduced our power to reach significance for the radial diffusivity values. Our follow-up analyses in male-only subgroups with FXS and IQ-CTLs revealed no significant between-group differences in fractional anisotropy, radial diffusivity and axial diffusivity. These results are consistent with a previous TBSS analysis in very young children with FXS, which reported no differences between males with FXS relative to a combined group of IQ-CTLs and neurotypical males.[13] However, it is likely that, in both cases, the sample size of the male groups resulted in lack of power to detect differences.

Within the FXS group, we found positive correlations between fractional anisotropy values and the Vineland Adaptive Behavior Scales' total score. In addition, this score was negatively correlated with radial diffusivity values. It is possible that within the FXS group, the specific influence of *FMR1* mutation is more uniform across participants, leading to detectable correlations between brain and behaviour. The lack of a comparable uniform influence in the IQ-CTL group might explain the absence of brain-behaviour correlations in this group. However, high fractional anisotropy and low radial diffusivity are usually interpreted as representing increased and more efficient structural connectivity (but could also represent other processes such as fewer crossing fibres).[37] Thus, the direction of the brain–behaviour correlation (positive correlation with fractional anisotropy and negative with radial diffusivity) was not thematically consistent with observed white matter differences between groups.

Beyond the specific genetic influence of the *FMR1* mutation on white matter microstructure putatively leading to increased fractional anisotropy and reduced radial diffusivity in the FXS group compared with the IQ-CTL group, common environmental processes can also influence white matter microstructure. In the mouse model for FXS, there is evidence that environmental enrichment influences both behaviour and white matter microstructures.[38,39] Exposure to environmental enrichment reduces FXS-related behaviours, such as hyperactivity, and synaptic abnormalities including reduced dendrite length and branching and immature-appearing cortical spines.[38,39] In children with FXS, advantageous environment leads to higher scores on the Vineland Adaptive Behavior Scales.[40] Thus, increased Vineland scores might reflect exposure of individuals to an 'enriched' home and family environment. We speculate that within the FXS group, this 'enriched' exposure could influence both Vineland Adaptive Behavior scores and white matter characteristics.

Limitations and conclusions

The current study has several limitations that should be noted. The absence of a neurotypical control group limits our ability to compare samples of FXS and IQ-CTL participants with neurotypical participants. This comparison would have allowed us to test the replicability of previous findings and compare those with current findings in our sample. Importantly, the IQ-CTL group consists of individuals with (currently) undifferentiated causes for their intellectual disability. Though this group provides a good representation of idiopathic intellectual disability in the general population, the heterogeneity of neurobiological risk factors among affected individuals could also affect the group-level white matter microstructure.

We included individuals with FXS from both genders because previous DTI studies have examined either females or males only, although studies within each gender suggest aberrant white matter microstructure in FXS.[4,5,13] Given the presence of a more severe phenotype in males with FXS relative to females, we also explored the effects of the *FMR1* full mutation in a male-only subgroup. We did not find significant group differences between males with FXS ($n = 15$) and the IQ-CTL group ($n = 13$). However, it is likely that the limited sample size of the male subgroups restricted our ability to draw gender-specific inferences. This underscores the need for larger neuroimaging studies in this highly affected subgroup of males with FXS. Finally, as in any DTI study, definitive conclusions about histology of white matter can only be derived from direct microscopic examination of biological tissue; thus, continued efforts should be made to study white matter microstructure in both humans and animal models with the *FMR1* full mutation.

In conclusion, to the best of our knowledge, this is the largest DTI study focusing on white matter microstructure in individuals with FXS and the only one to use a cognitively matched control group. Our findings demonstrate a consistent pattern of white matter microstructure aberrations in FXS across complementary methods of analysis (TBSS and TRACULA).The profile of white matter microstructure aberrations in FXS included increased fractional anisotropy and decreased radial diffusivity values compared with IQ-matched controls. The direction of fractional anisotropy and radial diffusivity value aberrations in FXS was opposite to that previously found between FXS and neurotypical controls (i.e. decreased fractional anisotropy and increased radial diffusivity and axial diffusivity in FXS[4,5]). Overall, our new findings underscore the need to control for cognitive ability when investigating white matter microstructure in neurodevelopmental disorders.

Tamar Green, MD, Center for Interdisciplinary Brain Sciences Research, Stanford University School of Medicine, Stanford, California, and Sackler Faculty of Medicine, Tel Aviv University, Tel Aviv; **Naama Barnea-Goraly**, MD, **Mira Raman**, MS, **Scott S. Hall**, PhD, **Amy A. Lightbody**, PhD, **Jennifer L. Bruno**, PhD, **Eve-Marie Quintin**, PhD, Center for Interdisciplinary Brain Sciences Research, Stanford University School of Medicine, Stanford, California; **Allan L. Reiss**, MD, Center for Interdisciplinary Brain Sciences Research, Department of Psychiatry and Behavioral Sciences, and Department of Radiology, Stanford University School of Medicine, Stanford, California.

Correspondence: Allan L. Reiss, Center for Interdisciplinary Brain Sciences Research, 401 Quarry Road, MC 5795, Stanford, CA 94305, USA. Email: areiss1@stanford.edu

First received 19 May 2014, final revision 12 Sep 2014, accepted 13 Oct 2014

https://doi.org/10.1192/bjp.bp.114.151654 Published online by Cambridge University Press

Funding

The National Institutes of Health (MH50047) provided grant support to A.L.R.; the Gazit-Globe Fund Fellowship Award provided support to T.G. The Canel Family Fund also supported this study.

Acknowledgements

The authors sincerely thank all of the families who kindly volunteered to participate.

References

1 Oostra BA, Chiurazzi P. The fragile X gene and its function. *Clin Genet* 2001; **60**: 399–408.

2 Crawford DC, Acuna JM, Sherman SL. FMR1 and the fragile X syndrome: human genome epidemiology review. *Genet Med* 2001; **3**: 359–71.

3 Reiss AL, Dant CC. The behavioral neurogenetics of fragile X syndrome: analyzing gene-brain-behavior relationships in child developmental psychopathologies. *Dev Psychopathol* 2003; **15**: 927–68.

4 Barnea-Goraly N, Eliez S, Hedeus M, Menon V, White CD, Moseley M, et al. White matter tract alterations in fragile X syndrome: preliminary evidence from diffusion tensor imaging. *Am J Med Genet B Neuropsychiatr Genet* 2003; **118B**: 81–8.

5 Villalon-Reina J, Jahanshad N, Beaton E, Toga AW, Thompson PM, Simon TJ. White matter microstructural abnormalities in girls with chromosome 22q11.2 deletion syndrome, Fragile X or Turner syndrome as evidenced by diffusion tensor imaging. *Neuroimage* 2013; **81**: 441–54.

6 Yu C, Li J, Liu Y, Qin W, Li Y, Shu N, et al. White matter tract integrity and intelligence in patients with mental retardation and healthy adults. *Neuroimage* 2008; **40**: 1533–41.

7 Saul RA, Tarleton JC. *FMR1-Related Disorders.* University of Washington, 2012 (http://www.ncbi.nlm.nih.gov/pubmed/20301558).

8 Brown V, Jin P, Ceman S, Darnell JC, O'Donnell WT, Tenenbaum SA, et al. Microarray identification of FMRP-associated brain mRNAs and altered mRNA translational profiles in fragile X syndrome. *Cell* 2001; **107**: 477–87.

9 Li C, Bassell GJ, Sasaki Y. Fragile X mental retardation protein is involved in protein synthesis-dependent collapse of growth cones induced by Semaphorin-3A. *Front Neural Circuits* 2009; **3**: 11.

10 Sidorov MS, Auerbach BD, Bear MF. Fragile X mental retardation protein and synaptic plasticity. *Mol Brain* 2013; **6**: 15.

11 Wang H, Ku L, Osterhout DJ, Li W, Ahmadian A, Liang Z, et al. Developmentally-programmed FMRP expression in oligodendrocytes: a potential role of FMRP in regulating translation in oligodendroglia progenitors. *Hum Mol Genet* 2004; **13**: 79–89.

12 Pacey LK, Xuan IC, Guan S, Sussman D, Henkelman RM, Chen Y, et al. Delayed myelination in a mouse model of fragile X syndrome. *Hum Mol Genet* 2013; **22**: 3920–30.

13 Haas BW, Barnea-Goraly N, Lightbody AA, Patnaik SS, Hoeft F, Hazlett H, et al. Early white-matter abnormalities of the ventral frontostriatal pathway in fragile X syndrome. *Dev Med Child Neurol* 2009; **51**: 593–9.

14 Berry-Kravis E, Hessl D, Abbeduto L, Reiss AL, Beckel-Mitchener A, Urv TK, et al. Outcome measures for clinical trials in fragile X syndrome. *J Dev Behav Pediatr* 2013; **34**: 508–22.

15 Sparrow SS, Ciccheti, DV, Balla, DA. *Vineland Adaptive Behavior Scales*, 2nd edn (Vineland-II). Pearson Assessments, 2006.

16 Tassone F, Pan R, Amiri K, Taylor AK, Hagerman PJ. A rapid polymerase chain reaction-based screening method for identification of all expanded alleles of the fragile X (FMR1) gene in newborn and high-risk populations. *J Mol Diagn* 2008; **10**: 43–9.

17 Lord C, Rutter M, Goode S, Heemsbergen J, Jordan H, Mawhood L, et al. Autism diagnostic observation schedule: a standardized observation of communicative and social behavior. *J Autism Dev Disorders* 1989; **19**: 185–212.

18 Wechsler D. *The Wechsler Intelligence Scale for Children,* 3rd edn. Psychological Corporation, 1991.

19 Wechsler D. *Wechsler Abbreviated Scale of Intelligence*. H.B. Company, 1999.

20 Sen PN, Basser PJ. A model for diffusion in white matter in the brain. *Bioph J* 2005; **89**: 2927–38.

21 Song SK, Sun SW, Ramsbottom MJ, Chang C, Russell J, Cross AH. Dysmyelination revealed through MRI as increased radial (but unchanged axial) diffusion of water. *Neuroimage* 2002; **17**: 1429–36.

22 Smith SM, Jenkinson M, Johansen-Berg H, Rueckert D, Nichols TE, Mackay CE, et al. Tract-based spatial statistics: voxelwise analysis of multi-subject diffusion data. *Neuroimage* 2006; **31**: 1487–505.

23 Smith SM, Jenkinson M, Woolrich MW, Beckmann CF, Behrens TE, Johansen-Berg H, et al. Advances in functional and structural MR image analysis and implementation as FSL. *Neuroimage* 2004; **23** (Suppl 1): S208–19.

24 Fischl B, van der Kouwe A, Destrieux C, Halgren E, Segonne F, Salat DH, et al. Automatically parcellating the human cerebral cortex. *Cereb Cortex* 2004; **14**: 11–22.

25 Yendiki A, Panneck P, Srinivasan P, Stevens A, Zollei L, Augustinack J, et al. Automated probabilistic reconstruction of white-matter pathways in health and disease using an atlas of the underlying anatomy. *Front Neuroinf* 2011; **5**: 23.

26 Behrens TE, Woolrich MW, Jenkinson M, Johansen-Berg H, Nunes RG, Clare S, et al. Characterization and propagation of uncertainty in diffusion-weighted MR imaging. *Mag Reson Med* 2003; **50**: 1077–88.

27 Wakana S, Caprihan A, Panzenboeck MM, Fallon JH, Perry M, Gollub RL, et al. Reproducibility of quantitative tractography methods applied to cerebral white matter. *Neuroimage* 2007; **36**: 630–44.

28 Smith SM, Jenkinson M, Johansen-Berg H, Rueckert D, Nichols TE, Mackay CE, et al. Tract-based spatial statistics: Voxelwise analysis of multi-subject diffusion data. *Neuroimage* 2006; **31**: 1487–505.

29 Nichols TE, Holmes AP. Nonparametric permutation tests for functional neuroimaging: a primer with examples. *Hum Brain Mapp* 2002; **15**: 1–25.

30 Wilcox RR. A heteroscedastic method for comparing regression lines at specified design points when using a robust regression estimator. *J Data Sci* 2013; **11**: 281–91.

31 Skranes J, Vangberg TR, Kulseng S, Indredavik MS, Evensen KA, Martinussen M, et al. Clinical findings and white matter abnormalities seen on diffusion tensor imaging in adolescents with very low birth weight. *Brain* 2007; **130**: 654–66.

32 Schmithorst VJ, Wilke M, Dardzinski BJ, Holland SK. Cognitive functions correlate with white matter architecture in a normal pediatric population: a diffusion tensor MRI study. *Hum Brain Mapp* 2005; **26**: 139–47.

33 Navas-Sanchez FJ, Aleman-Gomez Y, Sanchez-Gonzalez J, Guzman-De-Villoria JA, Franco C, Robles O, et al. White matter microstructure correlates of mathematical giftedness and intelligence quotient. *Hum Brain Mapp* 2013; **35**: 2619–31.

34 Campbell DS, Holt CE. Chemotropic responses of retinal growth cones mediated by rapid local protein synthesis and degradation. *Neuron* 2001; **32**: 1013–26.

35 Li C, Sasaki Y, Takei K, Yamamoto H, Shouji M, Sugiyama Y, et al. Correlation between semaphorin3A-induced facilitation of axonal transport and local activation of a translation initiation factor eukaryotic translation initiation factor 4E. *J Neurosci* 2004; **24**: 6161–70.

36 Hoeft F, Carter JC, Lightbody AA, Cody Hazlett H, Piven J, Reiss AL. Region-specific alterations in brain development in one- to three-year-old boys with fragile X syndrome. *Proc Natl Acad Sci USA* 2010; **107**: 9335–9.

37 Thomason ME, Thompson PM. Diffusion imaging, white matter, and psychopathology. *Annu Rev Clin Psychol* 2011; **7**: 63–85.

38 Lauterborn JC, Jafari M, Babayan AH, Gall CM. Environmental enrichment reveals effects of genotype on hippocampal spine morphologies in the mouse model of fragile X syndrome. *Cereb Cortex* 2015; **25**: 516–27.

39 Restivo L, Ferrari F, Passino E, Sgobio C, Bock J, Oostra BA, et al. Enriched environment promotes behavioral and morphological recovery in a mouse model for the fragile X syndrome. *Proc Natl Acad Sci USA* 2005; **102**: 11557–62.

40 Glaser B, Hessl D, Dyer-Friedman J, Johnston C, Wisbeck J, Taylor A, et al. Biological and environmental contributions to adaptive behavior in fragile X syndrome. *Am J Med Genet Part A* 2003; **117A**: 21–9.

https://doi.org/10.1192/bjp.bp.114.151654 Published online by Cambridge University Press